Performance of phase change materials for heat storage thermoelectric harvesting

M. E. Kiziroglou, A. Elefsiniotis, S. W. Wright, T. T. Toh, P. D. Mitcheson et al.

Citation: Appl. Phys. Lett. **103**, 193902 (2013); doi: 10.1063/1.4829044
View online: http://dx.doi.org/10.1063/1.4829044
View Table of Contents: http://apl.aip.org/resource/1/APPLAB/v103/i19
Published by the AIP Publishing LLC.

Performance of phase change materials for heat storage thermoelectric harvesting

M. E. Kiziroglou,[1,a)] A. Elefsiniotis,[2] S. W. Wright,[1] T. T. Toh,[1] P. D. Mitcheson,[1] Th. Becker,[2] and E. M. Yeatman[1]
[1]*Electrical and Electronic Engineering, Imperial College London, London SW7 2AZ, United Kingdom*
[2]*Electronics and Systems Integration, EADS, Munich, Germany*

(Received 28 May 2013; accepted 22 October 2013; published online 6 November 2013)

Heat storage energy harvesting devices have promise as independent power sources for wireless aircraft sensors. These generate energy from the temperature variation in time during flight. Previously reported devices use the phase change of water for heat storage, hence restricting applicability to instances with ground temperature above 0 °C. Here, we examine the use of alternative phase change materials (PCMs). A recently introduced numerical model is extended to include phase change inhomogeneity, and a PCM characterization method is proposed. A prototype device is presented, and two cases with phase changes at approximately −9.5 °C and +9.5 °C are studied. © *2013 AIP Publishing LLC*. [http://dx.doi.org/10.1063/1.4829044]

Recent advances in battery technology have raised expectations for energy density to values as high as 10 kWh/kg by employing technologies such as lithium-air electrodes.[1] New, patterned electrode materials are capable of reducing the charging time of high energy density batteries.[2] Nevertheless, in systems intended for long term operation, recharging or replacement is still necessary. Particularly for wireless sensor networks or devices operating in inaccessible locations, manual recharging, where an operator must visit a deployed device, incurs high costs and ultimately undermines the benefits of wireless technology. Energy harvesting is a rapidly developing technology which addresses this limitation by exploitation of local ambient energy.

A variety of energy sources and techniques have been proposed for harvesting, with suitability and performance largely depending on the application environment and specifications. A number of approaches have been proposed specifically for wireless sensor networks on aircraft, with the main energy sources available being vibration,[3] sunlight,[4] and radio frequency power transmission.[5]

Recently, a new thermoelectric energy harvesting approach was proposed which exploits the variation of ambient temperature with time.[6] A heat storage unit (HSU) is employed to capture heat, and the heat that flows in and out is transduced to electricity by a thermoelectric generator (TEG). A phase change material (PCM) is used in the HSU to boost its heat capacity and to increase the time lag between the internal and ambient temperature, and thus the temperature difference across the TEG. A review of PCMs and heat storage applications can be found in Ref. 7. A schematic of this device concept is shown in Fig. 1(a).

In previous papers, we have demonstrated that this new thermoelectric harvesting concept is particularly suitable for aircraft sensors.[8,9] However, while the energy output exceeds the requirements of state-of-the-art sensor nodes for appropriate device sizes, applicability has been limited to flight scenarios involving temperature profiles crossing 0 °C, because the PCM used was water. In this paper, we use a device of the type presented in Ref. 8 to evaluate PCMs with different phase-change temperatures, heat capacities, and heat conductivities. We study their performance by extending a recently introduced heat flow numerical model which allows the evaluation of phase change quality in terms of homogeneity, abruptness, and energy release.

An image of the prototype device is shown in Fig. 1(b). The HSU structure consists of a 60 × 30 × 30 mm aluminum box with internal thermal bridges, internal capacity of 30 cm^3, and a 2 mm thick polyurethane thermal insulation layer. Two TG12-2.5 Marlow TEGs with figure of merit $ZT = 0.72$ (at 27 °C) were used, each having a thermal resistance of 3.6 K/W and an electrical resistance of 5 Ω. The two TEGs were installed side-by-side, i.e., in parallel for heat flow, but were electrically connected in series to increase the total output voltage. Two types of PCM were studied, with thermal properties as presented in Table I and including 22% by weight of a thermal conductivity enhancement graphite additive, as provided by the supplier. The additive occupies a significant fraction of the PCM, and while increasing its thermal conductivity, it also reduces its specific heat. The corresponding properties of water are also shown for comparison with previously reported devices.[9,10] In all experiments, the amount of PCM used was 23 ml, which is 7 ml less than the container capacity in order to accommodate phase change expansion.

For performance characterization, the device was placed in an environmental chamber emulating temperature profiles corresponding to typical flights.[9] The temperature of the PCM, T_{in}, and the environmental temperature, T_{out}, were recorded using thermocouples (TC) located as shown in Fig. 1(a). Temperature gradients from the TC locations to the PCM and environment were found to be negligible. The combined voltage output of the two TEGs was measured while connected to a 10 Ω resistive load, matching the total internal resistance of the TEGs in order to maximise power transfer.

For performance evaluation, in a previous paper we introduced a numerical model in which the PCM temperature T_{in}, heat flow $\dot{Q}$, and open-circuit voltage output V_{oc}

a)m.kiziroglou@imperial.ac.uk

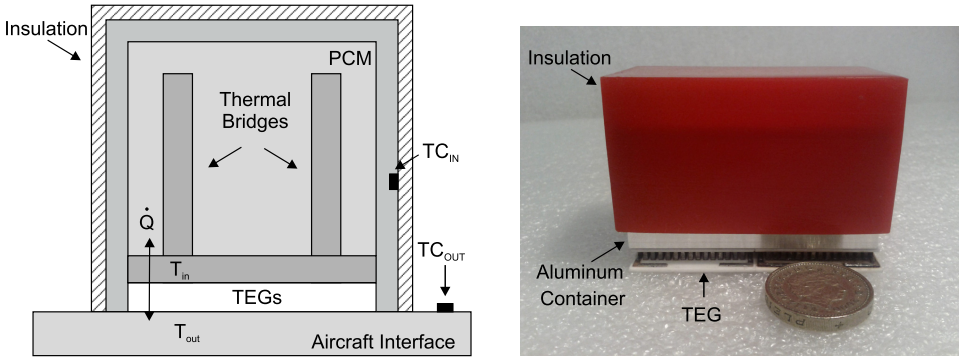

FIG. 1. (a) Schematic of the device concept. (b) A fabricated prototype as presented in Ref. 8.

response to a generic environmental temperature profile T_{out} can be calculated.[10] According to this model, if a device with HSU capacity C, HSU-to-environment heat resistance R, and TEG Seebeck coefficient α is in a state (n), then after a small time interval Δt it will be in a state $(n+1)$ such that

$$T_{in}(n+1) = \begin{cases} T_{in}(n) + (T_{out}(n) - T_{in}(n)) \times \dfrac{\Delta t}{RC} & \text{(NPC)} \\ T_{in}(n) & \text{(PC)}, \end{cases} \tag{1}$$

$$\dot{Q}(n+1) = \dot{Q}(n) + (T_{out}(n) - T_{in}(n)) \times \Delta t/R, \tag{2}$$

$$V_{OC} = \alpha \times (T_{out} - T_{in}), \tag{3}$$

where NPC indicates non-phase change and PC indicates phase change.

In this model, a uniform PCM temperature is assumed. As R is typically much larger than the heat resistance of the HSU interior, this assumption leads to negligible error during non-phase change operation. However, it yields a constant T_{in} during phase change, neglecting any inhomogeneity during the phase-change process. This leads to significant overestimation of energy output and inability to account for the phase change abruptness performance of different PCMs.

While commercial 2D and 3D simulators of phase change are available, they usually implement finite-element solutions of the heat equation, which are effective for specific sets of parameters but do not give an explicit indication of physical trends. In this respect, the introduction of phase change non-uniformity effects to the above model with good approximations would be advantageous in terms of simplicity, practicality, speed, and physical insight. An HSU typically includes an internal heat sink with fins as shown in Fig. 2(a). During phase changes, the phase change front propagates from the heat sink surface towards the PCM's core. If corner effects are neglected such that heat flux is homogeneous and perpendicular to the surface of the phase change front, then, at a given time t, the front will be at a distance $s(t)$ from the heat sink surface. The phase change will end when $s(t)$ reaches the surface of maximum distance W from the heat sink. This is illustrated in 2D in Fig. 2(b). If the fins contribute significantly to the heat sink internal area A, a constant phase change front surface area can be assumed and the problem is reduced to 1D, as shown in Fig. 2(c).

The solution of this moving boundary problem, known as the Stefan problem, involves the calculation of the temperature profile $T(x,t)$ and the phase change front position $s(t)$ from the heat equation. A similarity technique is used to reduce the partial differential equation to a single variable one.[11] The existence of an explicit solution depends on the imposed boundary and initial conditions.

In experimental measurements, T_{in} is usually measured as the temperature of the heat sink, which in the 1D Stefan problem of Fig. 2(c) corresponds to $T(x,0)$. As the variation of T_{in} during phase change is small compared to $T_{out} - T_{in}$, a constant heat flow $\dot{Q}_c = (T_{out} - T_{in})/R$ at $x = 0$ may be assumed. Under this boundary condition, no explicit solution exists. However, a quasi-stationary approximation can be obtained, provided that the latent heat of the PCM is much larger than the sensible heat that is absorbed during phase change.[12] This assumption is supported by the small T_{in} variation during phase change and also by the small specific to latent heat ratio that most PCMs exhibit. The corresponding solution is

$$s(t) = \frac{\dot{Q}_c}{\rho L A} t, \tag{4}$$

$$T(x,t) = T_{PC} + \frac{\dot{Q}_c}{kA}\left[\frac{\dot{Q}_c}{\rho L A} t - x\right], \tag{5}$$

where k, ρ, L, and T_{PC} are the PCM heat conductivity at its initial phase, the density, the latent heat, and the phase change temperature of the PCM, while A is the heat sink internal area. For maximization of energy harvesting, the temperature difference across the TEG is of great importance

TABLE I. List of investigated PCMs.

PCM name[a]	T_{PC} (°C)	ρ (kg/m^3)	L (kJ/kg)	c_p (J/kgK)	k (W/mK)
Water (solid)	0	917	334	2000	2.18
Water (liquid)		1000		4200	0.58
RBT[b] 10HCG	+9.5	825	165	2000	>0.2
RBT −9HCG	−9.5	825	236	2000	>0.2

[a]T_{PC}, ρ, L, c_p, and k are the phase change temperature, density, latent heat, thermal capacity, and thermal conductivity, respectively. In the PCM specifications, L was given for a 15 °C temperature range. The corresponding sensible heat has been subtracted from the L value.

[b]Rubitherm GmbH brand. Specifications do not include the k enhancement 22% by weight graphite additive.

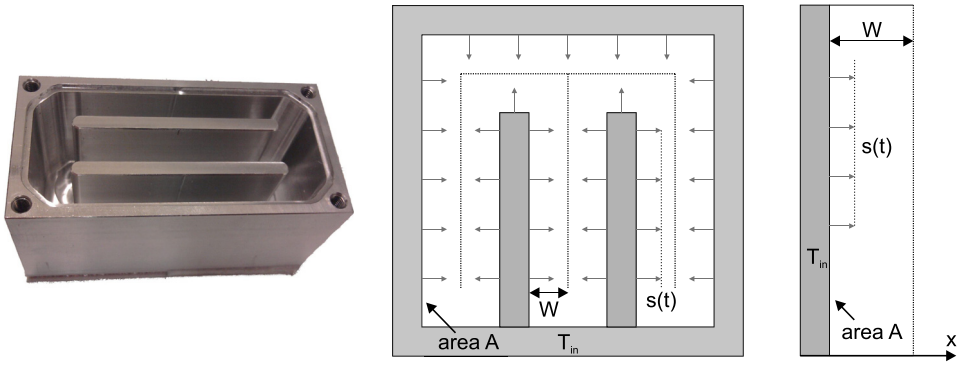

FIG. 2. (a) Photo of the HSU, (b) phase change propagation in 3D (2D illustration), (c) corresponding 1D model.

because it determines its efficiency. Hence, during phase change, the minimum possible drift of $T_{in} = T(0,t)$ is desirable. Equation (5) reveals and quantifies the importance of heat conductivity to the quality of phase change. A high k_{PCM} allows a more uniform phase change which in turn provides a more stable T_{in} and a higher overall efficiency. The latent heat, apart from its decisive role in the increase of heat storage density, is also very important to the phase change duration and quality and hence to efficiency. Finally, Eq. (5) also demonstrates the importance of the heat sink area A to the phase change homogeneity. A review of other approximate analytical and numerical approaches to the solution of the Stefan problem has been presented in Ref. 7.

This study can be incorporated into the numerical model of Eqs. (1)–(3) to account for phase change inhomogeneity and allow, by fitting with experimental results, characterization of the phase change performance of different PCMs. Setting $x = 0$ and taking the time derivative of Eq. (5), one obtains

$$\frac{dT_{in}}{dt} = \frac{\dot{Q}_c^{\,2}}{k\rho LA^2}. \tag{6}$$

By discretization and replacing $\dot{Q}_C$ by $(T_{out} - T_{in})/R$, the following equation for T_{in} is obtained:

$$T_{in}(n+1) = T_{in}(n) + \frac{(T_{out} - T_{in})^2}{R^2 k\rho LA^2}\Delta t \quad \text{(phase change)}. \tag{7}$$

Equation (7) can be used instead of a constant value during phase change in (1). This numerical model will be used in the next section to evaluate the performance of two different PCMs used with the developed prototype.

It is noted that the PCM thermal conductivity introduced in this model is the apparent conductivity that the PCM exhibits during phase change. It reflects the velocity of phase change propagation. In PCMs with abrupt phase change processes such as water, this should correspond to its thermal conductivity. In PCMs with gradual phase change or multistage phase change processes, it may be dominated by the speed and mobility of such processes. This parameter should be used with care in drawing conclusions about the properties of materials but offers a direct measure of phase change performance.

The device response with the PCM Rubitherm 10HCG is shown in Fig. 3, for a full temperature cycle between +20 °C and −20 °C. The non-phase change and phase change operation modes are clearly visible, with a considerable temperature drift during both phase changes. No supercooling is observed, as expected for an organic PCM.[7] The simulated device response, based on the experimentally measured T_{out} data, is also shown, using the simple model (model 1) and the model including phase change inhomogeneity (model 2). The nominal values of TEG resistance, PCM sensible heat capacity, PCM density, and phase change temperature (average, +9.5 °C) as given in the specifications were used. The as-measured PCM volume, 23 ml, and HSU internal area, 80 cm^2, were used. The latent heat and PCM thermal conductivity were the only fitting parameters. The fit shown corresponds to $L = 150 \pm 10$ kJ/kg and $k = 0.4 \pm 0.05$ W/mK. All other parameters were set according to the specifications of the materials and devices used. Higher heat conductivity is demonstrated in comparison with the additive-free Rubitherm PCM specifications (0.2 W/mK) at the expense of a 10% lower latent heat. These differences are expected as effects of the 22% by weight graphite additive. An accurate quantitative characterisation of the additive effect on L is avoided as the difference is close to the fitting (±10 kJ/kg) and specifications (±7%) error margins.

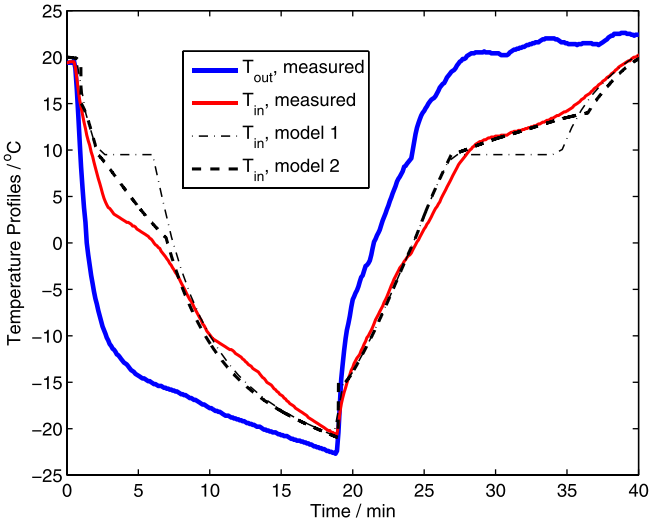

FIG. 3. Temperature response using the Rubitherm 10HCG PCM.

The heat conductivity appearing in Eqs. (5)–(7) is that of the PCM in the second phase of the transition being modelled. This means that for materials with different liquid and solid phase heat conductivities, such as water, a correspondingly different value is generally expected for the liquid-to-solid and solid-to-liquid phase changes. In addition, as it is used to fit the phase-change front propagation velocity, it incorporates nucleation, mass diffusion, and crystallization kinetics. Therefore, a value that deviates from the liquid/solid heat conductivities can appear. Nevertheless, a single k value for the fit in Fig. 3 was used for interpretation simplicity.

The TEG voltage output V_o on an $R_L = 10\,\Omega$ load and the corresponding cumulative energy, calculated as the time integral of power output $P_o = V_o^2/R_L$, are shown in Fig. 4. The results corresponding to models 1 and 2 are also shown in Fig. 4. A more accurate simulation from the inclusion of phase change inhomogeneity is clearly observed. The overestimation of output energy from both models is a consequence of the deviation of the experimentally observed solidification initiation temperature (4 °C) from the corresponding nominal value (9.5 °C) used in the models.

The device response with the RBT-9HCG PCM is shown in Fig. 5, for the same temperature cycle. This PCM case is relevant to winter flights from a northern airport, where both the ground and cruising ambient temperatures will be below 0 °C. Again, no supercooling but considerable temperature drift during phase change is observed. Simulation results corresponding to the two models are also shown, using the same nominal parameter values as those used in Fig. 3 but with a phase change temperature of −9.5 °C. By fitting the experimental response with the model, the latent heat and conductivity performance were found to be $L = 190 \pm 10$ kJ/kg and $k = 0.4 \pm 0.05$ W/mK, respectively. All other parameters were set according to specifications. The same k enhancement as with the RBT 10HCG is observed at the expense of a 20% L reduction, due to the additive. The corresponding voltage and cumulative energy profiles are shown in Fig. 6. A more accurate prediction of the device performance is obtained by using the model that includes phase change inhomogeneity. The

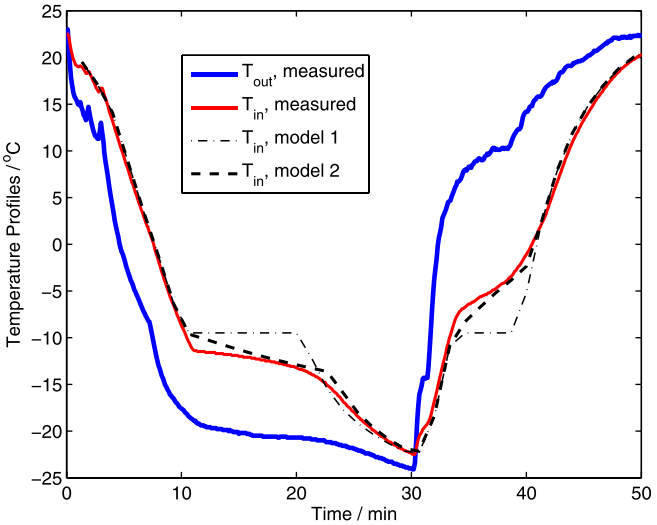

FIG. 5. Temperature response using the Rubitherm -9HCG PCM.

overestimation of output energy from both models is a consequence of the deviation of the experimentally observed phase change initiation temperature T_{PC} (−12 °C for solidification and −7 °C for liquefaction) from the corresponding nominal value (−9.5 °C) used in the models.

In this paper, the use of different PCMs in heat storage harvesting devices for aircraft sensors is proposed, extending their applicability to flight temperature profiles not necessarily traversing zero degrees. A numerical model including inhomogeneous phase change effects is introduced and a method of PCM performance characterization is proposed, based on their latent heat and phase change thermal conductivity properties.

It is found that further to the significance of L in energy density and of k in the minimization of ΔT loss, these parameters also reflect the abruptness of phase change and hence form a measure of PCM performance for heat storage harvesting devices. This is quantitatively expressed by Eq. (5). When fitting experimental data, the phase change thermal conductivity k of the PCM offers a measure of the phase change front mobility, encompassing by simplification multi-stage and gradual phase change processes.

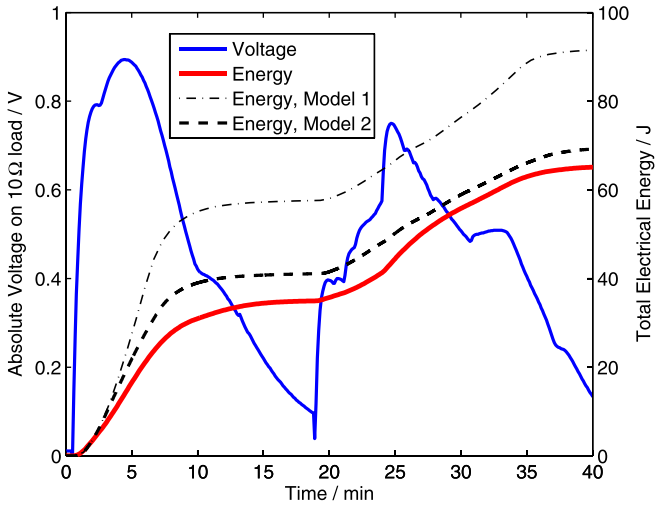

FIG. 4. Output voltage and energy response using the Rubitherm 10HCG PCM. The solid lines correspond to experimental data.

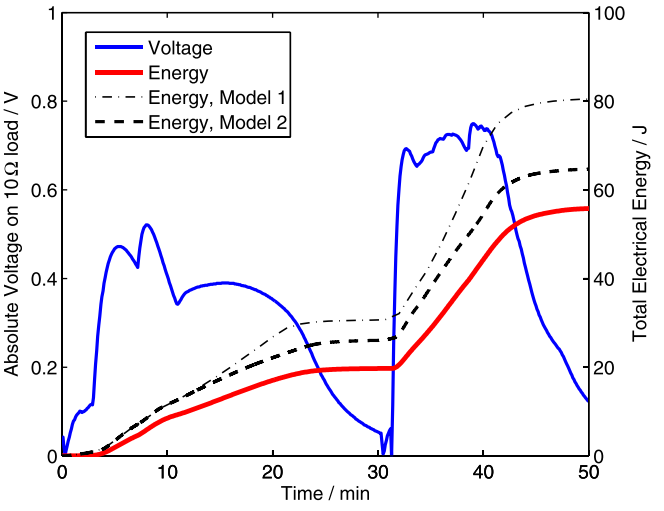

FIG. 6. Output voltage and energy using the Rubitherm -9HCG PCM. The solid lines correspond to experimental data.

Two devices using commercially available PCMs with phase change temperatures at approximately −9.5 °C and +9.5 °C are presented, demonstrating energy output of approximately 60 J from 23 ml of PCM, corresponding to an energy density of 3.1 J/g. This energy density is sufficient to cover the power requirements of state-of-the-art wireless sensor node systems for typical sensor node device sizes.

This work has been supported by the Clean Sky Joint Technology Initiative under the theme JTI-CS-2010-1-SFWA-01-016.

[1]J.-S. Lee, S. T. Kim, R. Cao, N.-S. Choi, M. L. Kyu, T. Lee, and J. Cho, Adv. Energy Mater. **1**(1), 34 (2011).
[2]X. Zhao, C. M. Hayner, M. C. Kung, and H. H. Kung, Adv. Energy Mater. **1**(6), 1079 (2011).
[3]S. Moss, A. Barry, I. Powlesland, S. Galea, and G. P. Carman, Appl. Phys. Lett. **97**(23), 234101 (2010).
[4]S. R. Anton, A. Erturk, and D. J. Inman, in *17th IEEE International Symposium on the Applications of Ferroelectrics*, Santa Fe, NM, USA (IEEE, 2008), p. 145.
[5]G. Liu, N. Mrad, G. Xiao, Z. Li, and D. Ban, in *Smart Materials, Structures & NDT in Aerospace* (CINDE, Montreal, Quebec, Canada, 2011).
[6]N. Bailly, J.-M. Dilhac, C. Escriba, C. Vanhecke, N. Mauran, and M. Bafleur, in *Proceedings of PowerMEMS*, Sendai, Japan (2008), p. 205. D. Samson, M. Kluge, Th. Becker, and U. Schmid, Sens. Actuators, A **172**(1), 240 (2011).
[7]A. Sharma, V. V. Tyagi, C. R. Chen, and D. Buddhi, Renewable Sustainable Energy Rev. **13**(2), 318 (2009).
[8]M. E. Kiziroglou, S. W. Wright, T. T. Toh, P. D. Mitcheson, Th. Becker, and E. M. Yeatman, *in PowerMEMS* (Atlanta, USA, 2012), p. 472.
[9]A. Elefsiniotis, D. Samson, Th. Becker, and U. Schmid, J. Electron. Mater. **42**(7), 2301 (2013).
[10]M. E. Kiziroglou, S. W. Wright, T. T. Toh, P. D. Mitcheson, T. Becker, and E. M. Yeatman, IEEE Trans. Ind. Electron. **61**(1), 302–309 (2014).
[11]P. DuChateau, *Introduction to Nonlinear PDEs* (Colorado State University, Fort Collins, CO, USA, 2013).
[12]V. Alexiades and A. D. Solomon, *Mathematical Modeling of Melting and Freezing Processes* (Taylor & Francis, Washington, DC, 1993).